LIMNOLOGY
and
OCEANOGRAPHY

ASLO

*Limnol. Oceanogr.* 61, 2016, S221–S237

doi: 10.1002/lno.10358

# Diffusive methane fluxes from Negro, Solimões and Madeira rivers and fringing lakes in the Amazon basin

**Pedro M. Barbosa,*[1,2] John M. Melack,[3] Vinicius F. Farjalla,[1,4] João Henrique F. Amaral,[5] Vinicius Scofield,[1,2] Bruce R. Forsberg[5]**

[1]Departamento de Ecologia, Instituto de Biologia, Universidade Federal do Rio de Janeiro, Rio de Janeiro, Rio de Janeiro, Brazil
[2]Programa de Pós-Graduação em Ecologia, Universidade Federal do Rio de Janeiro, Rio de Janeiro, Rio de Janeiro, Brazil
[3]Bren School of Environmental Science and Management, University of California, Santa Barbara, California, USA
[4]Laboratorio Internacional en Cambio Global (LINCGlobal)
[5]Environmental Dynamics Department, National Institute of Amazon Research (INPA), Manaus, Amazonas, Brazil

## *Abstract*

The first extensive set of measurements of methane concentrations and fluxes for the Negro River and its major tributaries combined with complementary data for the Solimões and Madeira rivers and several tributaries are presented and their temporal and spatial variations examined. Fluxes were measured using floating chambers, and dissolved $CH_4$ concentrations were measured by the headspace technique. In the Solimões basin, tributaries had higher fluxes when water levels were low; no statistical difference among periods for lakes and the main stem river was observed. In the Negro basin, rivers had higher fluxes with greater variations among rivers during high water than during low water based on fluxes calculated from the concentration gradient and modelled gas transfer coefficients. We estimate a regional methane emission of 0.31 Tg C $yr^{-1}$ for large river channels in the lowland Amazon basin.

Aquatic environments are an important component of the global carbon cycle and can be sources of both carbon dioxide ($CO_2$) and methane ($CH_4$) to the atmosphere. Methane is one of the final products of the degradation of organic matter (Bridgham et al. 2013) and is an important greenhouse gas (Forster et al. 2007). As concerns about climate change have increased in light of current warming rates, evaluating the sources of gases that can lead to warming is important. In particular, while wetlands and other inland waters are known to be the major natural source of methane (Melton et al. 2013), there is considerable uncertainty about the estimated amounts (Kirschke et al. 2013). Streams and rivers often contain methane and emit globally significant amounts (Stanley et al. 2015).

The lowland Amazon basin contains one of the world's largest complex of rivers, floodplains and wetlands. Covering a total floodable area of c. 800,000 $km^2$, these wetlands include seasonally inundated forests, open water environments (lakes and river channels) and floating herbaceous plants (Junk et al. 2011; Hess et al. 2015). Amazon aquatic habitats are an important source of $CH_4$ (Melack et al. 2004), and because of the size and heterogeneity of the region, there is considerable spatial and temporal variability in $CH_4$ fluxes (Bartlett et al. 1988; Crill et al. 1988; Devol et al. 1990; Engle and Melack 2000; Belger et al. 2011). Amazon floodplains are known to be sources of organic carbon and carbon dioxide to the river channels (Melack and Forsberg 2001; Melack and Engle 2009; Abril et al. 2014). Since methane is produced in anoxic environments, which are common in organic rich and thermally stratified lakes and wetlands and rare in river channels, floodplains could also act as a source of methane to rivers, as suggested by Borges et al. (2015a) for the Amazon and Congo rivers.

Because of the large spatial scale, variety of habitats and seasonal variability, measuring methane emissions in the Amazon basin is a challenge, and our understanding of the processes controlling emissions in this region is incomplete. The present study provides new information on seasonal differences in $CH_4$ concentrations and diffusive emissions to the atmosphere in a range of aquatic environments from three major tributaries of the Amazon River: the Negro,

*Correspondence: pebarbosa.limno@gmail.com

Additional Supporting Information may be found in the online version of this article.

**Special Issue:** Methane Emissions from Oceans, Wetlands, and Freshwater Habitats: New Perspectives and Feedbacks on Climate
Edited by: Kimberly Wickland and Leila Hamdan.

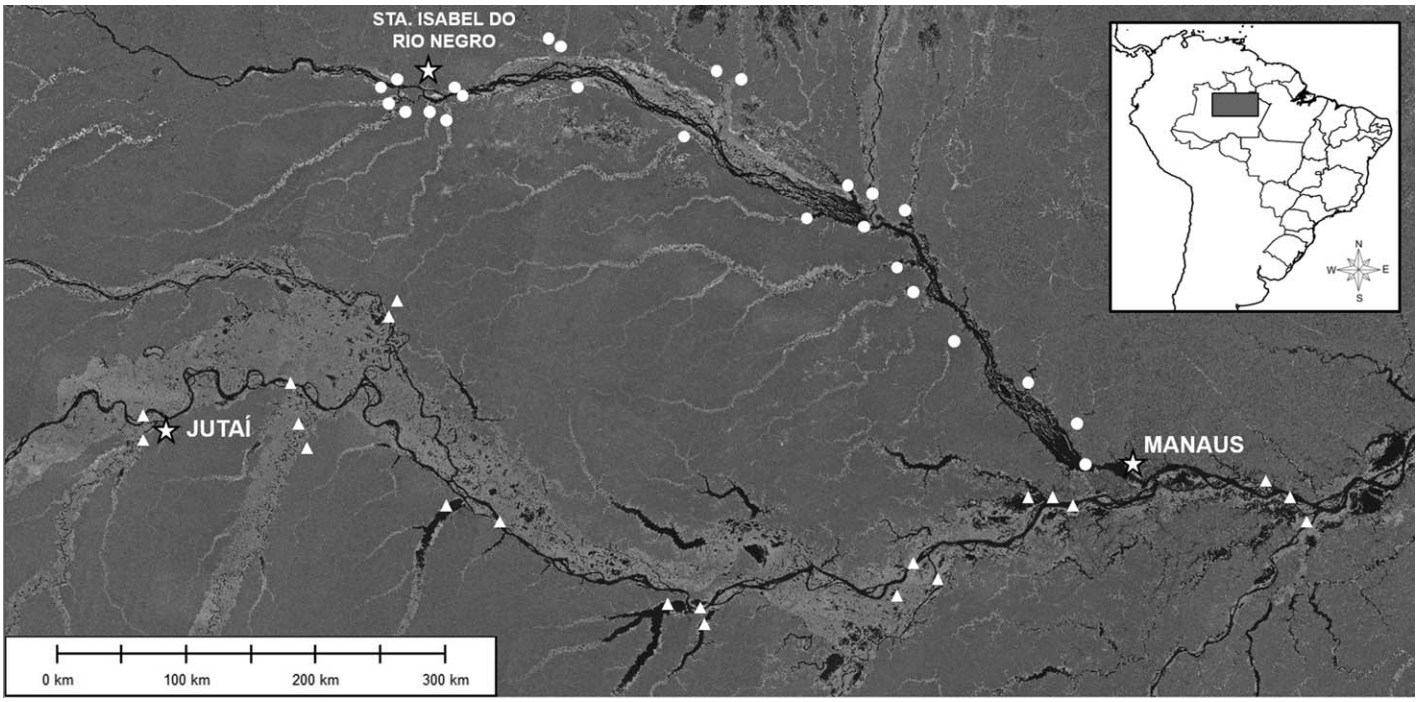


**Fig. 1.** The central portion of the Amazonian Basin, with the 46 sampling stations in the Negro (white circles) and Solimões/Madeira (white triangles) river basins. The background image is the Japanese Earth Resources Satellite-1 (JERS-1) mosaic displayed as a gray scale of radar backscatter (modified by B. Forsberg, unpubl.). The black shaded areas represent open water and the light grey represents floodable areas.

Solimões, and Madeira rivers as well as other rivers that feed these tributaries, and lakes bordering the Solimões River. These results are the first extensive data for the Negro basin, collected along a 700 km transect at 25 fluvial sites, including 4 stations in the mainstem of the Negro River, and in 21 of its tributaries. Additional measurements of limnological conditions provide ecological context.

## Methods

### Study area and sampling

The Amazon basin is the largest fluvial system in the world draining an area of approximately 6 million km$^2$ (Archer 2005) and is composed of a variety of aquatic habitats (Junk et al. 2011; Hess et al. 2015). High annual rainfall unevenly distributed through the year leads to large oscillations in river stage and discharge (Paiva et al. 2013). The study was performed in the central Amazon basin, along the Solimões, Madeira, and Negro rivers (Fig. 1). In the Negro basin, sampling and measurements were made at 4 stations along the Negro main stem, and in 21 of its major tributaries. In the Solimões/Madeira basin, 17 sites, including 10 floodplain lakes (open water) and 7 river channels, were sampled. Samples were collected during low water (*LW*) (November 2011), high water (*HW*) (May 2012), early falling water (*EFW*) (July 2012) and late falling water (*LFW*) (September 2012) in the Solimões/Madeira basin, and during low (December 2012) and high water (July 2011) in the Negro basin. All sampling and measurements were performed between 08:00 and 17:00 h, near the center of river channels and lakes. The Solimões/Madeira campaigns sampled environments along a 1100 km reach of the main stem, between Fonte Boa and the mouth of the Madeira River, including mainly rivers wider than 400 m and floodplain lakes (Fig. 1). The floodplain lakes include well-studied Calado (Melack and Forsberg 2001), oxbow lakes (Paupixuna), and large ria lakes (Tefé and Coari). In the Negro basin, sampling was done along a 700 km reach of the main stem, between Santa Isabel do Rio Negro and Manaus, and included mainly rivers wider than 100 m. The Solimões and Madeira rivers and most of their tributaries drain the Andes Mountains and their waters, rich in nutrients and sediments, are called "white waters." The Negro River and its tributaries drain the Precambrian Guiana shield and lowland forests, including extensive areas of hydromorphic podzols. Their waters, characteristically low in suspended sediments and high in dissolved organic carbon, are called "black waters."

### Limnological measurements

Water temperatures and dissolved oxygen concentrations were measured using a polarographic oxygen sensor (YSI 95, accuracy approximately 0.2 mg L$^{-1}$) and thermistor (YSI 95, accuracy 0.1°C). Water pH was measured with an electrode (Orion Star, Thermo Scientific; precision 0.1), and calibrated with 4.0 and 7.0 standards. Conductivity was measured using a portable meter (Orion Star, Thermo Scientific; accuracy 1 $\mu$S

$cm^{-1}$). Measurements were made at a depth of about 0.2 m in the rivers. During high and falling water periods, temperature and dissolved oxygen profiles were made every 0.5 m to within 0.5 m of the bottom in the lakes. Water for determination of chlorophyll *a* (Chl *a*), dissolved organic carbon (DOC), total suspended solids (TSS), total dissolved nitrogen (TDN) and total dissolved phosphorous (TDP) was also collected at all stations, and stored in insulated boxes until analysis. Water for Chl *a* was filtered through 0.7 $\mu$m glass fiber filters (Whatman GF/F) after a time period which never exceeded 8 h after the first sampling and the concentration of Chl *a* was determined spectrophotometrically using hot ethanol for pigment extraction and reading at 665 nm and 750 nm (Lorenzen 1967). Filtration was done in an improvised lab on a riverboat in dim light. Filters were frozen until analysis. DOC samples were filtered through precombusted (450–500°C for 1 h) glass fiber filters (Whatman GF/F). The filtered water was collected in borosilicate bottles, which were previously cleaned with HCl (10%), rinsed with deionized water and autoclaved, and stored at 4°C until analyzed using a total organic carbon analyzer (TOC-V Shimadzu, combustion catalytic oxidation at 680°C, non-dispersive infrared sensor). TSS was measured through differential weighing of GF/F glass fiber filters. TDN was measured through chemoluminescence with catalytic oxidation at 720° (TNM-1 Shimadzu), and TDP was determined according to Golterman et al. (1978) using sodium persulfate as an oxidant.

Wind speed was measured using a handheld anemometer (Kestel 3000) at 2 m above the water surface and facing into the wind for 5 min; the average speed given by the anemometer was recorded. Wind speed was normalized to a height of 10 m above the surface using the equation

$$\bar{u}_z = (u^*/\kappa)\ \ln\ (z/z_0), \tag{1}$$

where $\bar{u}_z$ is the mean wind speed (m $s^{-1}$) at height $z$, $u^*$ is the friction velocity (m $d^{-1}$), $\kappa$ is the von Karman's constant (0.4), and $z_0$ is the roughness length ($10^{-5}$ m, an intermediate value for water surfaces) (Oke 1988). Friction velocity was first calculated by rearranging Eq. 1 for $u^*$ and using the speed measured at 2 m as $\bar{u}_z$. An acoustic doppler current profiler (ADCP, RD Instruments, broadband, 600 kHz, 0.5 m bins) was used to measure current velocities and water depths and to calculate river discharges. ADCP transects were made laterally across each river channel through the sampling point.

Water from 0.2 m (all sites) below the surface and 0.5 m above the bottom (lakes only) was collected to determine dissolved $CH_4$ concentrations. One sample per depth, per site, was obtained. Samples from the sub-surface were collected directly with 60 mL polyethylene syringes, and a Van Dorn bottle was used for sampling at depth. The dissolved gas concentrations were determined using the headspace technique by equilibrating equal volumes (30 mL) of water and air in the sampling syringe (Hamilton et al. 1995). The equilibrated air was then transferred to a 20 mL glass serum vial, previously cleaned with HCl (10%) and rinsed with deionized water and stored at room temperature in dark until analyzed. A partition coefficient ($B_{aw}$) of 27 : 1 was used for calculation of dissolved $CH_4$ concentrations (Hansch and Leo 1979). For the temperatures at which we extracted the gases the range in partition coefficients would result in a variation of gas concentrations of less than 2% compared to the use of the single value we used. As atmospheric air was used for equilibration, the $CH_4$ atmospheric concentration was included in the water concentration calculation. According to mass conservation, the amount of gas existing in the syringe before equilibration is the same as after equilibration, so the water concentration was calculated through the following equation,

$$C_w + C_{air} = C_{w\ head} + C_{air\ head} \tag{2}$$

where $C_w$ is the $CH_4$ water concentration (ppmv), $C_{air}$ is the $CH_4$ atmospheric concentration (ppmv), $C_{air\ head}$ is the $CH_4$ headspace air concentration after equilibration (ppmv), and $C_{w\ head}$ is the $CH_4$ water concentration after equilibration (ppmv). $C_{w\ head} = C_{air\ head}/B_{aw}$.

Gas samples were analyzed using a gas chromatograph (Trace Ultra, Thermo Sci.) equipped with a flame ionization detector. The detector, injector and column temperatures were 200°C, 120°C, and 85°C, respectively. Calibration was done using standard gases of 10 ppmv and 50 ppmv, and the chromatograph was recalibrated after 25–30 samples, with the exception of the May samples when atmospheric air concentration was used for calibration. The detection limit was approximately 0.1 ppmv.

**Diffusive emission measurements**

Diffusive methane fluxes were measured using floating chambers except during HW in the Negro basin (see next section). The polyethylene chambers were covered with styrofoam for flotation, which also helped maintain stability. The chambers had an internal volume of 15 L and an internal area of 0.11 $m^2$. A 2 mm diameter polyethylene tube was inserted into the top of the chamber to permit gas sampling; a similar tube (3 m long) was inserted to equilibrate the inside and outside pressures. The edge of the chamber was about 0.06 m below the water surface, and the boat and chamber drifted while the measurements were being made in river channels, and were stationary when measuring in lakes. Measurements were done in the center of the sampled environments. During each measurement, four gas samples were collected from the chambers at 5 min intervals (0 min, 5 min, 10 min, and 15 min) using 60 mL polyethylene syringes and stored in 20 mL glass serum vials, previously cleaned with HCl (10%) and rinsed with deionized water, with high density butyl rubber stoppers until analyses (Devol et al. 1990).

Diffusive flux from chambers was estimated from a regression between deployment time and $CH_4$ concentration

inside the chamber; the slope of the regression is the amount of $CH_4$ emitted per unit of time. To determine the amount of gas emitted per unit of time and area, the slope was multiplied by the chamber volume, and divided by the chamber area. Only regressions with a regression coefficient above 0.75 were used in the flux calculations. Rarely, when jumps in methane concentrations occurred, likely caused by bubbles, the measurements were excluded. Measurements were usually made in duplicate using two chambers, although logistics sometimes resulted in use of one chamber.

**Modelled diffusive emissions**

In the Negro basin, diffusive fluxes were also calculated according to the following equation,

$$F = k\left(C_{\text{water}} - C_{\text{eq}}\right), \quad (3)$$

where $F$ is the $CH_4$ diffusive flux (mmol $m^{-2}$ $d^{-1}$), $k$ is the gas transfer coefficient (m $d^{-1}$), $C_{\text{water}}$ is the observed dissolved $CH_4$ concentration ($\mu$M) and $C_{\text{eq}}$ is the $CH_4$ concentration in equilibrium with the atmosphere. Although gas transfer velocities are influenced by several factors (MacIntyre et al. 1995), most parameterizations developed for flowing waters apply to streams and small rivers (Raymond et al. 2012). Alin et al. (2011) provide equations developed on large rivers in the Amazon and Mekong basins. They used floating chambers and measured fluxes of carbon dioxide; they noted that water velocity, depth and discharge data were not collected sufficiently close to the flux measurements to allow inclusion in their regressions. Beaulieu et al. (2012), working in the Ohio River (U.S.A.), found no statistically significant relation between $k$ for methane and water velocity; their relation with wind speed was similar to that reported by Alin et al. (2011). We also used our calculations of $k$ from chambers and our measurements of currents and winds for the Negro River and its tributaries to attempt to find relationships. We found a similar relation between wind speeds and $k$ values as Alin et al. (2011), and no statistically significant relation between current speed and $k$ values. The current speeds during the high water period were similar. One important characteristic of the lower reaches of the rivers sampled in the Negro basin is that the slope of the channels is very low and, at high water, the mainstem Negro River tends to retard flows of the tributaries creating backwater effects. Hence, we calculated gas transfer coefficients according to Alin et al. (2011), using the equation,

$$k_{600} = 4.46 + 7.11 \times U_{10}, \quad (4)$$

where $k_{600}$ is the $k$ value normalized to a temperature of 20°C and $U_{10}$ is the wind speed at 10 m height, calculated from wind speed measured at 2 m, as described above.

Equation 3 was also used to calculate $k$ values based on measurements of $F$ with floating chambers and associated gas concentrations. $K_{CH4}$ values were obtained with Eq. 5:

$$k_{CH4} = k(617/S_{CT})^{-0.5}, \quad (5)$$

where $S_{CT}$ is the Schimdt number for water temperature T (°C), calculated following (Wanninkhof 2014):

$$S_{CT} = 1909.4 - 120.78\ T + 4.1555T^2 - 0.080578\ T^3 + 0.00065777\ T^4 \quad (6)$$

**Statistical analyses**

We used generalized linear models to evaluate the factors influencing $CH_4$ concentrations and emissions to the atmosphere. All analyses were performed using the package *nlme* (Pinheiro et al. 2015; R Statistical Software version 3.2.2, <www.r-project.org>). Using $CH_4$ concentrations, we evaluated the main and interactive effects of river basin (Negro, Solimões/Madeira), sampled period (LW and HW), environment type (tributaries, main stem) and environmental variables (e.g., DOC concentration, dissolved oxygen concentration, pH) on $CH_4$ water concentrations. To meet normality and homocedasticity assumptions, $CH_4$ concentrations were cubic root-transformed. We built models containing all variables and interactions between variables and used an averaging procedure to identify the best fitting model (functions "*aictab*" and "*evidence*" in the *Aiccmodavg* package; Mazerolle 2015). Best fitting models were those that had the smallest AICc scores (Burnham and Anderson 2004). We also ran generalized linear models using the Solimões/Madeira data with four sampled periods (HW, LW, EFW, LFW) and three environment types (lakes, tributaries, and main stem). We performed contrast analyses between categories within factors using the package *lsmeans* (Lenth and Herva 2015).

Generalized linear models were used for each basin using emissions from chambers for the Solimões/Madeira basin and emissions obtained from Eq. 3 for the Negro basin. For each basin, we evaluated the main and interactive factors of sampled periods, environmental type (tributaries and mainstem), and environmental variables on $CH_4$ emissions. To meet normality and homocedasticity assumptions, $CH_4$ emission data from Solimões/Madeira basin were log-transformed, and $CH_4$ emission data from Negro basin were cubic root-transformed.

## Results

**Limnological characteristics**

Physical and chemical conditions varied both between and within basins (Supporting Information Tables 1–4). In the Negro basin (Supporting Information Table 1), pH was acidic, varying between 4.5 (Aiuana, Daraá, Preto, and Tea rivers) and 7 (Branco River) during high water, and between 4.2 and 6.2 during low water (Apunã and Branco rivers, respectively). DOC concentrations varied between 1.2 mg $L^{-1}$ (Branco R., low water) and 34.6 mg $L^{-1}$ (Daraá River, low water), and averaged 16.6 mg $L^{-1}$ at low water and 11.1 mg

$L^{-1}$ at high water. Conductivity was slightly higher during the high water period (averages of 16 $\mu$S $cm^{-1}$ and 14 $\mu$S $cm^{-1}$ for high and low water, respectively). Water temperatures were above 25°C, and were similar between low and high water periods, varying from 25.2°C (Daraá River during high water) to 31.5°C (Arrirará River during low water). Rivers were more oxygenated during the low water period, when dissolved oxygen concentrations varied from 4.1 mg $L^{-1}$ to 7.4 mg $L^{-1}$ (Uneiuxi and Jufari rivers, respectively). During the high water period, values ranged from 1.2 mg $L^{-1}$ to 5.3 mg $L^{-1}$ (Cuiuni and Daraá rivers, respectively). Total suspended sediment concentrations were low, ranging between 2 mg $L^{-1}$ and 34 mg $L^{-1}$, and Chl *a* concentrations varied from 0.1 $\mu$g $L^{-1}$ to 12.1 $\mu$g $L^{-1}$. Total dissolved nitrogen ranged from 0.1 mg $L^{-1}$ (Branco R., low water) to 4.7 mg $L^{-1}$ (Daraá R., high water), and averaged 0.6 mg $L^{-1}$ and 0.4 mg $L^{-1}$ for high and low water, respectively. Total dissolved phosphorus varied between 0.01 $\mu$M (Caurés R., low water) to 5.1 $\mu$M (Negro R., station 1, high water), and averaged 0.63 $\mu$M and 0.34 $\mu$M for high and low water, respectively. Discharge varied from 40 $m^3$ $s^{-1}$ to 12,830 $m^3$ $s^{-1}$ in the low water period (Daraá and Negro 4, respectively) and from 30 $m^3$ $s^{-1}$ to 57,170 $m^3$ $s^{-1}$ during high water (Paoari and Negro 4, respectively). Current velocity varied little between low and high water periods (averages of 0.35 m $s^{-1}$ and 0.4 m $s^{-1}$, for low and high waters, respectively), with the highest value recorded in the Negro River main stem (station 2) during the high water period (1.2 m $s^{-1}$), and the lowest value (0.02 m $s^{-1}$) in the Apuaú River, also during high water.

In the Solimões and Madeira basins, pH ranged from 4.6 (Curupira L.) to 8.2 (Mamiá L), both during the low water period. Conductivity ranged from 6 $\mu$S $cm^{-1}$ (Coari L., high water) to 121 $\mu$S $cm^{-1}$ (Juruá R., late falling water). DOC concentrations varied between 2.1 mg $L^{-1}$ (Madeira R., low water) to 10.2 mg $L^{-1}$ (Juruá R., high water), and were similar between rivers and lakes of the basin (average of 4.4 mg $L^{-1}$ and 5.3 mg $L^{-1}$ for rivers and lakes, respectively). Water temperatures were above 26.8°C. Surface water temperatures were higher in the lakes (Supporting Information Table 2) than the rivers (Supporting Information Table 3), with the highest value (32.9°C) recorded in late falling water period (Coari L.). Dissolved oxygen concentrations were also higher in lakes than rivers, and values ranged between 1.9 mg $L^{-1}$ (Cabaliana L., high water) to 8.3 mg $L^{-1}$ (Mamiá L., low water). In rivers, concentrations ranged from 0.6 mg $L^{-1}$ (Jutaí R., high water) to 7.2 mg $L^{-1}$ (Madeira R., low water). Chlorophyll concentrations in lakes ranged from 0.9 $\mu$g $L^{-1}$ (Paupixuna L. early falling water) to 79.9 $\mu$g $L^{-1}$ (Ananás L., low water), while in rivers values ranged from 0.01 $\mu$g $L^{-1}$ (Jutaí R., high water) to 16 $\mu$g $L^{-1}$ (Jutaí R., late falling water). TSS in rivers ranged from 7 mg $L^{-1}$ (Jutaí R., high water) to 188 mg $L^{-1}$ (Juruá R., low water). The concentrations of total dissolved nitrogen were similar between rivers and lakes (averages of 0.38 mg $L^{-1}$ and 0.32 mg $L^{-1}$ for rivers and lakes, respectively), varying from 0.14 mg $L^{-1}$ (Tefé L., low water), to 0.69 mg $L^{-1}$ (Cabaliana L., low water). The same trend was observed for total dissolved phosphorus, with similar values for rivers and lakes (averages of 0.55 $\mu$M and 0.51 $\mu$M for rivers and lakes, respectively). The values ranged between 0.04 $\mu$M (Jutaí R., low water), to 1.85 $\mu$M (at Ananás R., high water). The majority of sampled lakes were thermally and chemically stratified during high and falling water periods. Rivers discharge ranged from 5.120 $m^3$ $s^{-1}$ to 169,000 $m^3$ $s^{-1}$ during high water (Juruá and Amazonas rivers, respectively) (Supporting Information Tables 3, 4), and from 1.580 $m^3$ $s^{-1}$ to 41,580 $m^3$ $s^{-1}$ at low water (Jutaí and Amazonas rivers, respectively). Rivers from this basin had higher current velocities than Negro basin rivers, with an average value of 1.3 m $s^{-1}$. Values ranged from 0.36 m $s^{-1}$ (Jutaí R., LFW), to 2.6 m $s^{-1}$ (Solimões R., station 2). The high water period had the highest values (average of 1.56 m $s^{-1}$), while the late falling water period had the lowest values (average of 0.88 m $s^{-1}$).

**Dissolved methane concentrations**

Subsurface methane concentrations were variable in time and space, and supersaturated with respect to atmospheric equilibrium (Tables 1-5). Overall, dissolved $CH_4$ concentration ranged from 0.003 $\mu$M in the Juruá and Solimões (station 4) rivers to 10.3 $\mu$M in the Jutaí River during high water. In the Negro R. basin, $CH_4$ concentrations in the main stem varied between 0.03 $\mu$M and 0.41 $\mu$M (both in HW period), with a median value of 0.14 $\mu$M (Table 4), while tributary concentrations ranged from 0.06 $\mu$M (Apuaú R., LW period), to 9.0 $\mu$M (Jaú R., HW period), with a median value of 0.41 $\mu$M (Table 5).

For the lowland Amazon basin (Negro and Solimões/Madeira basins), the variables that best explained $CH_4$ water concentration were the river basin sampled ($t = -3.1$; $p = 0.003$), the environment type (tributary or main stem, $t = 3.0$; $p = 0.004$), water temperature ($p = 0.004$), and the interaction between river basin and sampled period ($t = -2.0$; $p = 0.0004$). The best model explained approximately 55% of the variation on $CH_4$ concentration. This model included dissolved oxygen ($t = -0.6$; $p = 0.55$) and dissolved organic carbon ($t = -0.05$; $p = 0.96$) concentrations, although these variables were not individually significant. The sampled rivers in the Negro basin had higher $CH_4$ water concentrations than rivers in the Solimões/Madeira basins ($t = -3.1$; $p = 0.003$) (Fig. 2).

For the Solimões/Madeira basins, which also included the floodplain lakes, the variables that best fitted the model were the sampled period ($t = 2.6$; $p = 0.01$), the environment type ($t = -3.5$; $p = 0.0009$), water temperature ($t = -4.2$; $p = 0.0001$), dissolved oxygen ($t = -0.5$; $p = 0.62$) and dissolved organic carbon ($t = -1.2$; $p = 0.26$) concentrations, and pH ($t = -0.02$; $p = 0.98$), although these three last

**Table 1.** Coordinates of each sampling site, dissolved $CH_4$ concentrations in surface water and $CH_4$ fluxes measured using floating chambers, for stations in the Solimões/Amazon mainstem, during the periods of low (LW), high (HW), early falling (EFW), and late falling water (LFW). The highest value of each column is marked with a plus, and the lowest value is marked with an asterisk.

| | Coordinates | | [$CH_4$] $\mu$M | | | | Chamber Flux mmol $m^{-2}$ $d^{-1}$ | | | |
|---|---|---|---|---|---|---|---|---|---|---|
| Environment | Lat. | Long. | LW | HW | EFW | LFW | LW | HW | EFW | LFW |
| Solimões 1 | −2.69254 | −66.90504 | 0.14 | BD | 0.10 | 0.10$^+$ | NS | 0.50 | 0.79 | 0.75 |
| Solimões 2 | −2.500855 | −65.841664 | NS | 0.19$^+$ | 0.08 | 0.10 | 7.20$^+$ | 0.05* | 0.18 | 0.92$^+$ |
| Solimões 3 | −3.45615 | −64.46024 | 0.04* | BD | 0.33$^+$ | 0.06 | NS | 0.43 | 1.05$^+$ | 0.17* |
| Solimões 4 | −4.02417 | −62.99251 | 0.05 | 0.003* | 0.02 | 0.04 | NS | 0.90$^+$ | 0.06 | 0.28 |
| Solimões 5 | −3.81479 | −61.6366 | NS | 0.01 | 0.05 | 0.06 | NS | 0.21 | 0.16 | BD |
| Solimões 6 | −3.32125 | −60.55513 | 0.04 | 0.01 | 0.01* | BD | NS | NS | 0.01* | 0.57 |
| Amazonas | −3.24495 | −58.97293 | 0.93$^+$ | 0.01 | 0.02 | 0.02* | 3.25* | NS | 0.67 | 0.23 |
| Average | | | 0.24 | 0.04 | 0.09 | 0.06 | 5.23 | 0.42 | 0.42 | 0.49 |
| Median | | | 0.05 | 0.01 | 0.05 | 0.06 | 5.23 | 0.43 | 0.18 | 0.43 |

**Table 2.** Coordinates of each sampling sites, dissolved $CH_4$ concentration on surface water and $CH_4$ flux measured using floating chamber, for the tributaries of the Solimões River basin, during the periods of low (LW), high (HW), early falling (EFW), and late falling water (LFW). The highest value of each column is marked with a +, while the lowest value is marked with a *. BD: bellow detection limit for the method. The maximum, minimum, average, and median values for each column are presented in the bottom.

| | Coordinates | | [$CH_4$] $\mu$M | | | | Chamber Flux mmol $m^{-2}$ $d^{-1}$ | | | |
|---|---|---|---|---|---|---|---|---|---|---|
| Environment | Lat. | Long. | LW | HW | EFW | LFW | LW | HW | EFW | LFW |
| Jutaí | −2.83828 | −66.92907 | 0.72$^+$ | 10.34$^+$ | 0.07 | 0.55$^+$ | 52.11$^+$ | 23.29$^+$ | 0.22 | 242.32$^+$ |
| Juruá | −2.696 | −65.79713 | 0.19 | 0.003* | 0.05 | 0.14 | 0.36 | 0.45 | 0.09* | 0.25 |
| Japurá | −2.04071 | −65.21194 | 0.28 | 0.02 | 0.08$^+$ | 0.25 | 21.98 | 0.40* | 0.35 | 1.17 |
| Purus | −3.84996 | −61.39021 | 0.14* | 0.04 | 0.04* | 0.08* | 0.89 | BD | 0.12 | 0.19* |
| Madeira | −3.54031 | −58.91169 | 0.70 | 0.02 | BD | 0.09 | 0.34* | 0.41 | 0.42$^+$ | 0.31 |
| Average | | | 0.41 | 2.08 | 0.06 | 0.22 | 15.14 | 6.14 | 0.24 | 48.85 |
| Median | | | 0.28 | 0.02 | 0.06 | 0.14 | 0.89 | 0.43 | 0.22 | 0.31 |

variables were not individually significant. The interaction between the sampled period and the environment type was marginally significant ($t = 1.9$; $p = 0.06$). This model explained approximately 44% of the $CH_4$ concentrations. Methane concentrations tended to be higher when the water level was low, with a significant difference between low and high water ($z = -2.7$; $p = 0.007$; median values of 0.17 $\mu$M and 0.02 $\mu$M for LW and HW, respectively), and between LFW and HW ($z = -1.2$; $p = 0.03$), with the LFW median value 5 times higher (0.10 $\mu$M) (Fig. 3) (Tables 1-3). No statistical difference was detected between lakes and tributaries or between tributaries and the main stem river. For the lakes in the Solimões basin and the Solimões main stem, no statistical difference was found between sampled periods. For tributaries a significant difference for $CH_4$ dissolved concentration was found between the LW and HW periods ($z = -2.4$; $p = 0.01$), with the median value for LW 14 times higher than the HW one (0.28 $\mu$M and 0.02 $\mu$M for LW and HW, respectively) (Table 2).

Methane concentrations measured near the bottom of lakes (Table 3) were often more than one order of magnitude higher than subsurface waters. Values ranged from 0.02 $\mu$M in Paupixuna (early falling water) and Cabaliana lakes (high water) to 218 $\mu$M in L. Calado. The lakes had more dissolved $CH_4$ in the bottom waters during the high water period (median, 10.6 $\mu$M). The late falling water period had median $CH_4$ near-bottom water concentration (0.58 $\mu$M) almost 2 times higher than during early falling water (0.3 $\mu$M), and had the highest near-bottom water value (218 $\mu$M) in L. Calado. Cabaliana L. had the lowest subsurface value (0.02 $\mu$M), during the high water period.

On average, there was a 60% difference between subsurface and near-bottom $CH_4$ concentrations. In half of the cases this percentage was above 95%. Mamiá L. had the

**Table 3.** Coordinates of each sampling site, dissolved $CH_4$ concentrations in surface water, dissolved $CH_4$ concentrations in bottom water, and $CH_4$ fluxes measured using floating chambers for the lakes of the Solimões basin, during the periods of low (LW), high (HW), early falling (EFW), and late falling water (LFW). The highest value of each column is marked with a plus, and the lowest value is marked with an asterisk. NS: not sampled due to logistical issues; BD: below detection.

| | Coordinates | | [$CH_4$] Surface $\mu$M | | | | [$CH_4$] Bottom $\mu$M | | | | Chamber Flux mmol $m^{-2}$ $d^{-1}$ | | | |
|---|---|---|---|---|---|---|---|---|---|---|---|---|---|---|
| Environment | Lat. | Long. | LW | HW | EFW | LFW | LW | HW | EFW | LFW | LW | HW | EFW | LFW |
| Ananás | −3.92034 | −61.70023 | 2.35$^+$ | 0.73$^+$ | NS | 0.95 | NS | 0.64 | NS | 0.76 | 5.71$^+$ | 1.03$^+$ | NS | 11.53 |
| Cabaliana | −3.30481 | −60.72203 | 0.01* | 0.01* | 0.004* | 0.02 | NS | 0.02* | 0.09 | 0.58 | 0.06* | BD | 0.09 | 2.86 |
| Calado | −3.30868 | −60.57206 | 0.26 | 0.01* | 0.08 | 0.39 | NS | 19.49 | 74.06 | 218.63$^+$ | 1.14 | 0.54 | 3.48 | 18.60$^+$ |
| Coari | −4.04877 | −63.18697 | 0.07 | BD | 0.02 | 0.03 | NS | NS | 0.05 | 0.06 | 0.26 | BD | 23.81$^+$ | BD |
| Curupira | −2.0332 | −65.19695 | NS | 0.33 | 0.12 | 0.41 | NS | 104.08$^+$ | 52.96 | 2.00 | NS | 0.69 | 0.48 | 0.58 |
| Mamiá | −4.0883 | −62.98385 | 0.11 | 0.01 | 0.08 | 2.88$^+$ | NS | 97.78 | 78.51$^+$ | 179.36 | 0.30 | 0.83 | BD | 13.17 |
| Paupixuna | −2.75412 | −65.76936 | 0.37 | 0.04 | 6.79$^+$ | NS | NS | 0.07 | 0.02* | NS | 0.56 | 0.03* | 0.36 | NS |
| Tefé | −3.32423 | −64.73872 | 0.06 | BD | 0.01 | 0.07 | NS | 10.62 | 0.06 | 0.09 | 0.25 | BD | 0.06* | 0.08* |
| Tia Dora | −3.22866 | −59.07502 | 0.40 | 0.22 | 0.25 | 0.11 | NS | 0.21 | 0.30 | 0.06* | 2.79 | BD | 2.07 | 10.74 |
| Average | | | 0.45 | 0.19 | 0.92 | 0.61 | – | 29.11 | 25.75 | 50.19 | 1.38 | 0.62 | 4.34 | 8.22 |
| Median | | | 0.19 | 0.04 | 0.08 | 0.25 | – | 5.63 | 0.19 | 0.67 | 0.43 | 0.69 | 0.48 | 10.74 |

**Table 4.** Coordinates of sampling sites, dissolved $CH_4$ concentrations in surface water, $CH_4$ fluxes measured using floating chambers, and $CH_4$ fluxes estimated using Eq. 3, for the Negro River (except HW for chamber measurements; $n = 1$). The highest value of each column is marked with a plus, and the lowest value is marked with an asterisk.

| | Coordinates | | [$CH_4$] $\mu$M | | Chamber flux mmol $m^{-2}$ $d^{-1}$ | Equation 3 mmol $m^{-2}$ $d^{-1}$ | |
|---|---|---|---|---|---|---|---|
| Environment | Lat. | Long. | LW | HW | LW | LW | HW |
| Negro 1 | −0.40808 | −65.20611 | 0.13* | 0.03* | 0.86 | 0.95* | 0.20* |
| Negro 2 | −0.48713 | −64.81695 | 0.21$^+$ | 0.41$^+$ | 4.28$^+$ | 1.57$^+$ | 0.55 |
| Negro 3 | −1.40184 | −61.87655 | 0.14 | 0.08 | 1.59 | 1.32 | 0.22 |
| Negro 4 | −3.06241 | −60.27483 | 0.14 | 0.37 | 0.83* | 1.14 | 2.00$^+$ |
| Average | | | 0.15 | 0.23 | 1.89 | 1.24 | 0.74 |
| Median | | | 0.14 | 0.23 | 1.23 | 1.23 | 0.39 |

largest differences, with subsurface waters containing only 0.001% of the bottom concentration at high water, 0.1% at early falling water and less than 2% in late falling water. In contrast, Paupixuna L. had subsurface $CH_4$ concentration more than 300 times higher than bottom water concentration during the early falling water season (6.8 $\mu$M and 0.02 $\mu$M for subsurface and bottom water concentrations, respectively). These higher concentrations in surface water were unusual and were observed on only four other occasions.

### Diffusive flux of methane

A total of 196 flux chamber measurements were made, of which 142 (72%) were above the minimum $R^2$ value adopted for the regression ($R^2 \geq 0.75$). Due to analytical problems during the high water campaign in the Negro basin, measurements from chambers were not available. The chamber fluxes were variable among environments and sampled periods (Tables 1-5).

Riverine chamber fluxes in the Solimões basin ranged from 0.01 mmol $m^{-2}$ $d^{-1}$ during early falling water (Solimões R.) to 242 mmol $m^{-2}$ $d^{-1}$ during late falling water (Jutaí R.) (Tables 1, 2). In the main stem Solimões/Amazonas, diffusive fluxes ranged from 0.01 mmol $m^{-2}$ $d^{-1}$ (EFW period) to 7.2 mmol $m^{-2}$ $d^{-1}$ (EFW period) (Table 1). Lacustrine fluxes ranged from 0.03 mmol $m^{-2}$ $d^{-1}$ to 23.8 mmol $m^{-2}$ $d^{-1}$, in Cabaliana and Coari lakes, respectively (Table 3; Fig. 5). In general, the chamber measurements were skewed toward the smaller fluxes, as can be seen in the relative frequency distribution of the $Log_{10}$ $CH_4$ flux (Fig. 4). Cabaliana L. had fluxes below the median during all sampled periods, and registered the lowest value within lakes during the low water period (0.006 mmol $m^{-2}$ $d^{-1}$). The fluxes in Solimões main stem were significantly lower than the lacustrine

**Table 5.** Coordinates of each sampling site, dissolved $CH_4$ concentrations in surface water, $CH_4$ fluxes measured using floating chambers (except for HW, $n = 1$), and $CH_4$ fluxes estimated using Eq. 3, for the tributaries of the Negro River, during the periods of low water and high water. The highest value of each column is marked with an asterisk.

| | Coordinates | | [$CH_4$] $\mu$M | | Chamber flux mmol $m^{-2}$ $d^{-1}$ | Equation 3 mmol $m^{-2}$ $d^{-1}$ | |
|---|---|---|---|---|---|---|---|
| Environment | Lat. | Long. | LW | HW | LW | LW | HW |
| Aiuana | −0.59274 | −64.92058 | 0.44 | 0.25 | 0.79 | 1.49 | 0.43 |
| Apuaú | −2.50751 | −60.79432 | 0.06 | 0.54 | 0.36 | 0.57 | 2.32 |
| Aracá | −0.39649 | −62.93258 | 0.21 | 1.35 | 0.23 | 0.75 | 6.61 |
| Arirarrá | −0.49608 | −63.58785 | 0.32 | 0.81 | 0.30 | 1.37 | 2.00 |
| Branco | −1.30996 | −61.86639 | 0.26 | 0.47 | 1.01 | 2.66 | 1.37 |
| Caurés | −1.32896 | −62.32114 | 0.17 | 0.79 | 0.75 | 1.67 | 3.32 |
| Cuieiras | −2.82715 | −60.49924 | 0.33 | 0.69 | 0.37 | 0.72 | 2.88 |
| Cuiuni | −0.76862 | −63.15117 | 0.41 | 1.88 | 2.24 | 1.23 | 12.39 |
| Daraá | −0.43753 | −64.7604 | 0.31 | 1.47 | 0.50 | 1.01 | 5.37 |
| Demini | −0.3965 | −62.88757 | 0.23 | 0.20 | 0.71 | 0.85 | 1.36 |
| Jaú | −1.89486 | −61.53462 | 0.26 | 9.00 | 0.50 | 1.43 | 33.25 |
| Jauaperi | −1.33552 | −61.5891 | 0.27 | 0.53 | 0.77 | 1.45 | 0.80 |
| Jufari | −1.09921 | −62.06573 | 0.21 | 0.38 | 0.42 | 1.08 | 2.96 |
| Marauia | −0.38587 | −65.20145 | 1.06 | 0.60 | 3.85 | 3.71 | 1.62 |
| Paoari | −0.14469 | −64.094 | 0.42 | 0.77 | 1.07 | 1.98 | 1.21 |
| Preto | −0.10303 | −64.1158 | 0.26 | 0.27 | 0.21 | 1.01 | 0.94 |
| Puduari | −2.14386 | −61.2832 | 0.35 | 3.72 | 1.95 | 2.71 | 27.84 |
| Tea | −0.53572 | −65.17575 | 0.42 | 5.04 | 0.76 | 1.39 | 16.07 |
| Tupé | −3.04407 | −60.25476 | 0.25 | 0.21 | 1.36 | 0.65 | 0.27 |
| Uneiuxi | −0.60765 | −65.13699 | 0.47 | 0.99 | 0.72 | 2.12 | 2.96 |
| Unini | −1.64856 | −61.63081 | 0.17 | 1.75 | 0.40 | 0.59 | 10.51 |
| Urubaxi | −0.52657 | −64.82219 | 0.30 | 1.56 | 0.54 | 1.82 | 2.66 |
| Average | | | 0.33 | 1.51 | 0.90 | 1.47 | 6.33 |
| Median | | | 0.29 | 0.78 | 0.72 | 1.38 | 2.77 |

diffusive fluxes ($z = 2.2$; $p = 0.03$), and marginally lower than the tributary diffusive fluxes ($z = -1.9$; $p = 0.06$) (Fig. 5). The coefficient of variation (CV) for paired chambers in the main stem ranged from 8% (Solimões 4, LFW) to 45% (Solimões 2, EFW), in the tributaries ranged from 6% (Jutaí R., HW) to 84% (Purus R. EFW), and in lakes varied from 0% (Coari and Mamiá) to 94% at Paupixuna L. (HW) (see Supporting Information Table 5). The high values are uncommon, and the average CV for all chamber fluxes measured in the Solimões basin was 27%. The model that best explains the variation in diffusive flux for the Solimões/Madeira basin included $CH_4$ concentration ($t = 2.5$; $p = 0.02$), environment type ($t = 2.3$; $p = 0.03$), water temperature ($t = 3.9$; $p = 0.0003$), dissolved organic carbon concentration ($t = 0.98$; $p = 0.33$), although individually not significant, and the sampled period, which was marginally significant ($t = -1.9$; $p = 0.06$). The model explains about 38% of the variation in $CH_4$ diffusive flux.

Main stem Negro River LW chamber fluxes varied between 0.83 and 4.28 mmol $m^{-2}$ $d^{-1}$ (LW period) (Table 1); the one HW lower mainstem chamber flux was 0.38 mmol $m^{-2}$ $d^{-1}$. In the Negro River basin, tributary LW chamber fluxes ranged from 0.21 (Preto R.) to 3.85 mmol $m^{-2}$ $d^{-1}$ (Marauia R.) (Table 2): the one HW tributary chamber flux was 0.36 mmol $m^{-2}$ $d^{-1}$ in L.Tupe, a small ria lake draining into the lower Negro R. Mainstem LW chamber fluxes had CVs ranging between 3% and 20% (average of 13%), and tributary LW CVs ranged between 5% (Branco R.) and 63% (Jauperi R.) with an average of 24% (see Supporting Information Table 6).

Wind speeds in Negro basin were low during both sampled periods (averages of 1.6 m $s^{-1}$ and 1 m $s^{-1}$ for low and high water, respectively). The highest value was registered on the Branco River during low water (3.5 m $s^{-1}$), while the lowest value was near zero, registered on the Preto River, also during low water.

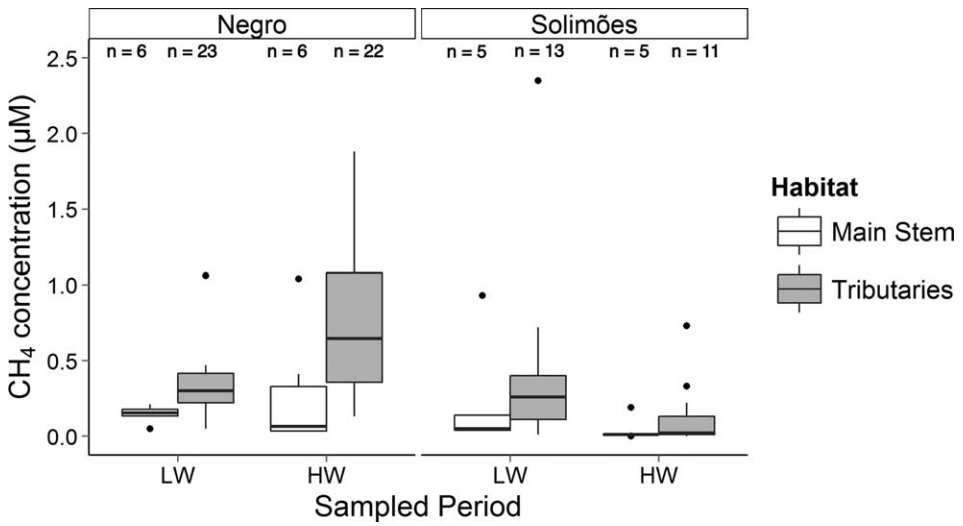


**Fig. 2.** Dissolved $CH_4$ concentrations ($\mu$M) in the Negro and Solimões/Madeira river basins, during low water (LW) and high water (HW) periods. The boxplot central lines correspond to the median of the distribution, and the vertical lines corresponds to the first and third quartiles (the 25th and 75th percentiles). Values above 2.5 $\mu$M ($n = 6$), were excluded from the figure.

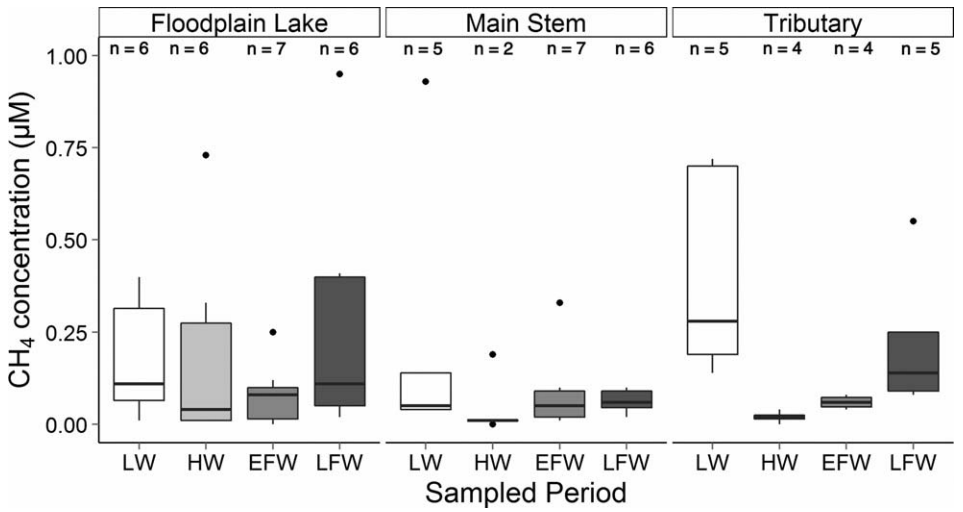


**Fig. 3.** Dissolved $CH_4$ concentrations ($\mu$M) in the floodplain lakes, tributaries and main stem of the Solimões/Madeira river basins, during the low water (LW), early falling water (EFW), late falling water (LFW), and high water (HW) periods. The boxplot central lines correspond to the median of the distribution, and the vertical lines correspond to the first and third quartiles (the 25th and 75th percentiles). Values above 1.0 $\mu$M ($n = 4$), were excluded from the figure.

Diffusive fluxes were calculated using winds speeds, methane concentrations and Eqs. 3 and 4 for HW and LW periods for rivers in the Negro basin (Tables 4, 5). For the LW period fluxes measured with chambers were also available and allow comparison. For the main stem Negro River, median fluxes determined by the two techniques were the same (1.23 mmol $m^{-2}$ $d^{-1}$), reflecting, in part, the similar average $k$ values (38 cm $h^{-1}$ as $k_{CH4}$ from chambers and 35 cm $h^{-1}$ as $k_{600}$ from Eq. 4 from Alin et al. 2011). For tributaries, median modelled fluxes (1.38 mmol $m^{-2}$ $d^{-1}$) were slightly higher than the fluxes from chambers (0.72 mmol $m^{-2}$ $d^{-1}$), reflecting, in part, higher average modelled $k$ values (21 cm $h^{-1}$ as $k_{600}$) vs. those from chambers (14 cm $h^{-1}$ as $k_{CH4}$).

Modelled methane fluxes in the mainstem Negro River ranged from 0.2 mmol $m^{-2}$ $d^{-1}$ to 2 mmol $m^{-2}$ $d^{-1}$ (both values during the HW period) (Table 4) and in tributaries ranged from 0.57 mmol $m^{-2}$ $d^{-1}$ to 3.71 mmol $m^{-2}$ $d^{-1}$ at LW period (median of 1.38 mmol $m^{-2}$ $d^{-1}$), and from 0.27 mmol $m^{-2}$ $d^{-1}$ to 33.25 mmol $m^{-2}$ $d^{-1}$ at HW (median of 2.77 mmol $m^{-2}$ $d^{-1}$) (Table 5).

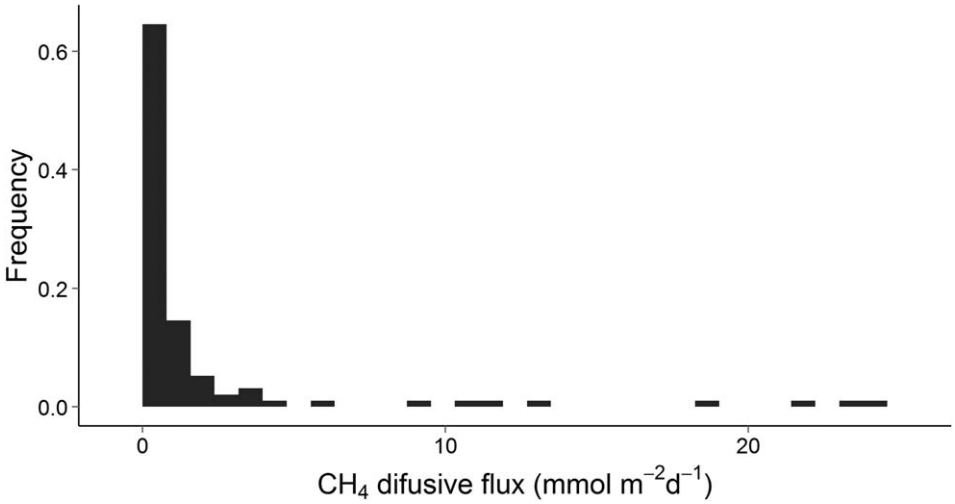


**Fig. 4.** Frequency distribution (%) of diffusive fluxes (mmol $m^{-2}$ $d^{-1}$) measured using floating chambers (n = 194). The values from Jutaí R. at LW, and LFW, as outliers were removed from the figure.

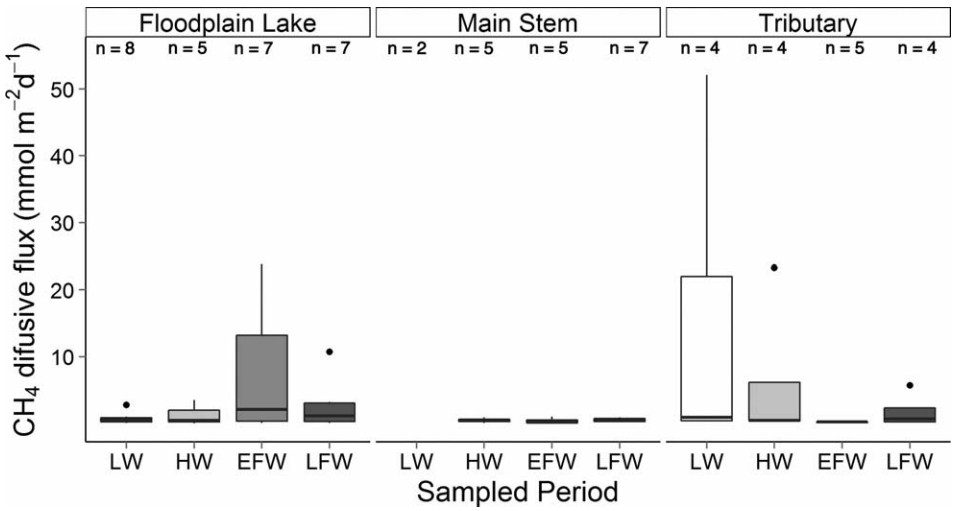


**Fig. 5.** Diffusive methane chamber fluxes (mmol $m^{-2}$ $d^{-1}$) in the floodplain lakes, tributaries and mainstem of the Solimões/Madeira river basins, during the low water (LW), early falling water (EFW), late falling water (LFW), and high water (HW) periods. The boxplots central lines correspond to the median of the distribution, and the vertical lines correspond to the first and third quartiles (the 25th and 75th percentiles). Single value above 55 mmol $m^{-2}$ $d^{-1}$ was excluded from the figure.

## *Discussion*

### Temporal and spatial differences

Temporal and spatial variability in both dissolved $CH_4$ concentrations and fluxes to the atmosphere are evident in our results and those of others (Melack et al 2004). As found by Crill et al. (1988) and Devol et al. (1990) working in floodplain lakes, lacustrine and river channel diffusive fluxes were influenced by a few high values. Hence, median values better represent the dataset than means.

The riverine chamber fluxes measured in our study (median of 0.41 mmol $m^{-2}$ $d^{-1}$) were similar to those calculated by Sawakuchi et al. (2014) working on lower Solimões and Amazonas rivers (medians of 0.26 mmol $m^{-2}$ $d^{-1}$ and 0.37 mmol $m^{-2}$ $d^{-1}$ for the Solimões and Amazonas main stems, respectively). The average surface concentrations of $CH_4$ along the 30 km reach below Tucuruí, Samuel and Curuá-Una dams were 1.3 $\mu$M, 1.5 $\mu$M, and 1.1 $\mu$M and the average emissions were 8.5 mmol $m^{-2}$ $d^{-1}$, 1.7 mmol $m^{-2}$ $d^{-1}$, and 1.1 mmol $m^{-2}$ $d^{-1}$, respectively (Kemenes et al. 2016). Downstream of Balbina dam, on the Uatumã R., the average concentration of methane was 36 $\mu$M and the average emission was 140 mmol $m^{-2}$ $d^{-1}$ (Kemenes et al. 2007),

**Table 6.** Channel areas, $CH_4$ flux per unit área and total flux for different lowland basins of the Amazon basin.

| Lowland Basin | Channel area $km^2$ | Flux mmol $m^{-2}$ $d^{-1}$ | Total flux Gg C $yr^{-1}$ |
|---|---|---|---|
| Amazon (basin-wide) | 52380 | | 306 |
| Xingu (Sawakuchi et al. 2014) | 3850 | 1.8 | 30.4 |
| Tapajós (Sawakuchi et al. 2014) | 5180 | 0.6 | 13.6 |
| Madeira (present study) | 4390 | 0.4 | 7.6 |
| Purus (present study) | 980 | 0.4 | 1.7 |
| Juruá (present study) | 470 | 0.3 | 0.6 |
| Japurá (present study) | 2050 | 0.6 | 5.4 |
| Solimões/Amazon (present study) | 17060 | 1.6 | 119.6 |
| Negro basin (present study) | 6730 | 2.0 | 59.0 |
| Summed above (not including Amazon basin-wide) | 40710 | | 238 |

values far above other rivers without hydroelectric reservoirs, with the exception of our measurement in the Jutaí R., which is statistically an outlier in our dataset.

Borges et al. (2015b) reported methane evasion from large African rivers based on measurements of gas concentrations and estimates of *k* values as done by Raymond et al. (2013): Congo R. (18.5 mmol $m^{-2}$ $d^{-1}$); Zambezi (13.6 mmol $m^{-2}$ $d^{-1}$) and Niger (0.6 mmol $m^{-2}$ $d^{-1}$). Emissions in their moderate-sized African rivers ranged from 0.6 mmol $m^{-2}$ $d^{-1}$ to 28.5 mmol $m^{-2}$ $d^{-1}$. Teodoru et al. (2015) reported emissions from the Zambezi system and noted how Victoria Falls, in a manner analogous to releases through turbines in hydroelectric reservoirs (Abril et al. 2005; Kemenes et al. 2007, 2016), is a hotspot for methane evasion, releasing as much as the Zambezi R. would emit over a 33 km reach 600 m wide.

Among sampled periods in lakes, no significant differences in chamber fluxes and concentrations were found. Devol et al. (1990) reported a similar result for lakes near Manaus in the central Amazon basin. Our lacustrine fluxes ranged from 0.06 mmol $m^{-2}$ $d^{-1}$ to 23.8 mmol $m^{-2}$ $d^{-1}$. Melack et al. (2004) used a flux from lakes of $3.2 \pm 0.5$ mmol $m^{-2}$ $d^{-1}$ for the regional extrapolation. Chamber diffusive fluxes in lakes measured in the Orinoco basin had a median of 0.48 mmol $m^{-2}$ $d^{-1}$ (Smith et al. 2000) and in the Pantanal an average of 0.74 mmol $m^{-2}$ $d^{-1}$ (Bastviken et al. 2010).

During mixing events, methane from the hypolimnion of lakes can reach the surface, and be emitted. Such an event was reported by Engle and Melack (2000), working at L. Calado, during a rare passage of a frontal cool air mass. This natural cooling event, recently discussed by Caraballo et al. (2014), could be the reason for the high dissolved $CH_4$ concentration (6.8 $\mu$M) measured in the surface of Paupixuna L. during the measurements in EFW. During this period we also measured low surface oxygen concentrations (2.5 mg $L^{-1}$), indicative of a mixing event.

In rivers of the Solimões/Madeira basin, higher dissolved $CH_4$ concentrations and fluxes occurred during the low water period, with fluxes and concentrations diminishing as water levels rose. This trend was also observed when separating main stem and tributary sites. Similar results were found by Sawakuchi et al. (2014), working on large rivers in the lower Amazon basin.

Richey et al. (1988) combined measurements of dissolved methane concentrations in the mainstem Solimões/Amazonas River with estimates of air–water gas-exchange rates (Devol et al. 1987) to determine a diffusive evasion rate of 0.2 mmol $m^{-2}$ $d^{-1}$, which is similar to 0.17 mmol $m^{-2}$ $d^{-1}$ determined by Bartlett et al. (1990) during rising water using floating chambers. Median $CH_4$ fluxes found in the present study for the Solimões mainstem were 0.43 mmol $m^{-2}$ $d^{-1}$ during HW and LFW and 0.18 mmol $m^{-2}$ $d^{-1}$ during EFW.

Sawakuchi et al. (2014) reported measurements of methane concentrations and fluxes in the lower main stem Solimões/Amazonas rivers and five tributaries (lower Negro, Madeira, Tapajos, Xingu, and Para) based on floating chambers. Sixteen of the 34 sites were sampled during low and high water. Dissolved, near-surface methane concentrations ranged from 0.02 $\mu$M to 0.5 $\mu$M, which are in the range of the values measured in the present study. Diffusive fluxes ranged from 0.01 mmol $m^{-2}$ $d^{-1}$ to 18.6 mmol $m^{-2}$ $d^{-1}$ with the higher fluxes in the Tapajós, Xingu, and Amazonas rivers. Their data for the Negro and Solimões rivers were based on sites near Manaus and represent only the lowest reaches of these rivers. In the present study, we sampled six stations in the Solimões main stem, and four stations along the Negro main stem. The Negro R. had higher dissolved $CH_4$ concentrations, especially during the HW period, in comparison to the Solimões R.

Several authors working at tropical floodplains, such as the Orinoco (Smith et al. 2000), the Pantanal (Bastviken et al. 2010), and the Amazon (Devol et al. 1988, 1990),

found a strong relation between gas water concentration and its flux to the atmosphere. In the Solimões basin $CH_4$ concentration and water temperature were positively related to $CH_4$ diffusive flux ($p = 0.0003$). As discussed by Stanley et al. (2015), the relation between water temperature and $CH_4$ emission is often ambiguous. For example, Smith et al. (2000), working in the Orinoco floodplain found no relation between these two variables. Environment type was also related to $CH_4$ diffusive emissions in the Solimões basin. The Solimões main stem had lower $CH_4$ diffusive fluxes and concentrations than the lakes and tributaries. Sawakuchi et al. (2014) found higher fluxes in the tributaries, when compared to the mainstem Amazonas River.

Mechanisms of methane production are the same in rivers and lakes, although factors that regulate $CH_4$ production and its emission to the atmosphere appear to differ. The relation between the river channels and the adjacent floodplain has been shown to be important for several elements and processes. Mayorga et al. (2005) suggested that materials from the floodplain could be responsible for sustaining the high respiration rates found in Amazonian rivers. Moreira-Turcq et al. (2013) estimated a mass balance for the particulate organic carbon that supported the importance of interaction between rivers and lakes. Furthermore, Abril et al. (2014), working on the Amazon River floodplain, suggested that much of the $CO_2$ in the main stem river is derived from the adjacent floodplain indirectly, by improving the availability of carbon, or directly through the respiration in roots. They estimated that Amazonian wetlands export half their primary production to adjacent waters, part of which can support a large percentage of inland water $CO_2$ evasion. The interaction between rivers channels and the surrounding floodplain for the $CH_4$ dynamics is not well understood. Richey et al. (1988), Bartlett et al. (1990) and Devol et al. (1994) reported a gradient of increasing methane toward the margins of the Solimões R., indicating the floodplain could act as a source of $CH_4$ to the river. Sawakuchi et al. (2014), in contrast, inferred little interaction between the river and the adjacent floodplain based on their data. Borges et al. (2015a) suggest that the dynamics of $CH_4$ in the Amazon and Congo rivers is related to the hydrological connectivity between the fringing wetlands and the river channels. Further work that incorporates measurements and models of river-floodplain exchanges, such as reported by Rudorff et al. (2014a,b), is warranted.

In comparison to the floodplains along the Solimões/Amazonas River, there is a lack of information on $CH_4$ emissions from the Negro basin. We estimated a median emission of diffusive fluxes for the Negro basin tributaries, based on calculations with Eq. 4 at high and low water, as 2.8 mmol $m^{-2}$ $d^{-1}$ and 1.4 mmol $m^{-2}$ $d^{-1}$, and for the main stem Negro R. as 0.4 mmol $m^{-2}$ $d^{-1}$ and 1.2 mmol $m^{-2}$ $d^{-1}$, respectively. Based on measurements with floating chambers in the Jaú basin Rosenqvist et al. (2002), calculated a mean annual emission of methane from flooded forest of 1.9 mmol $m^{-2}$ $d^{-1}$. Upper Negro interfluvial wetlands are a mosaic of emergent grasses, sedges, shrubs and palms with shallow permanent water or seasonal flooding. Belger et al. (2011), working in interfluvial wetlands of the Negro basin, measured methane uptake on unflooded lands, evasion from flooded areas as diffusive and ebullitive fluxes with chambers and funnels, and as transport through rooted plants. Based on annual emission from two interfluvial wetlands, Belger et al. (2011) estimated average $CH_4$ emission from wetland areas of 1.8 mmol $m^{-2}$ $d^{-1}$ for $CH_4$. Jati (2013) made monthly measurements of methane flux with floating chambers in 80 wetlands near Boa Vista (Roraima); the mean emission value from his results was about 0.8 mmol $m^{-2}$ $d^{-1}$ for $CH_4$.

**Gas transfer velocities and occurrence of ebullition**

In the open waters included in our study, exchange of methane between surficial water and overlying atmosphere can occur by diffusive processes and by ebullition. Diffusive exchange depends on the concentration gradient between air and water and on physical processes at the interface, usually parameterized as a gas transfer velocity ($k$). In the lakes along the Solimões R. that we sampled, $k_{CH4}$ values, derived from our chamber measurements, averaged 13.3 cm $h^{-1}$; a few anomalous values were excluded. Rudorff et al. (2011) used three different models of $k$, and Polsenaere et al. (2013) applied an eddy covariance technique to calculate fluxes and $k$ values. Rudorff et al. (2011) reported gas transfer coefficients that take into account wind as well as heating and cooling, which were on the order of 10 cm $h^{-1}$. Polsenaere et al. (2013) reported $k$ values averaging $12.2 \pm 6.7$ cm $h^{-1}$. Based on floating chambers deployed in Balbina Reservoir, Kemenes et al. (2011) calculated $k$ values with an average of about 12 cm $h^{-1}$.

At low wind speeds, which occurred during most of our measurements, empirically derived relationships between wind speeds and $k$ have large uncertainty and considerable scatter (Cole and Caraco 1998; Crusius and Wanninkhof 2003; Alin et al. 2011). Recent work by MacIntyre et al. (2010) has shown that during low winds, nocturnal buoyancy flux can be a major source of turbulence, a process not well represented by most empirical methods. In our study, for both the Negro and the Solimões basins, wind velocities were low, with the majority below 3 m $s^{-1}$. The few events of higher speed winds (above 2.5 m $s^{-1}$) coincide with fluxes above the median when using Eq. 3.

In flowing waters, values of $k$ for Amazon waters have been derived using $^{222}Rn$ and from methane fluxes measured in floating chambers, (Devol et al. 1987; Alin et al. 2011; Kemenes et al. 2011; Rasera et al. 2013). Devol et al. (1987) combined their Rn based values with a dissolved oxygen balance and other empirical analyses to estimate a likely $k$ value for the main stem Amazon River of about 19 cm $h^{-1}$. The range of $k$ values reported by Alin et al. (2011) and Rasera et al. (2013) for

rivers in the Amazon (1.2–31.6 cm $h^{-1}$), are quite similar. For the Uatumã River below Balbina Reservoir, Kemenes et al. (2011) reported average *k* values of 10.5 cm $h^{-1}$.

Our estimated *k* values (expressed as $k_{CH4}$) derived from our chamber measurements, differed among the rivers sampled. Negro basin rivers ranged from 2.8 cm $h^{-1}$ to 37 cm $h^{-1}$ with mainstem stations higher (average 26 cm $h^{-1}$, excluding one anomalous value) than tributaries (average, 14 cm $h^{-1}$). The combination of the mainstem Solimões/Madeira sites and Solimões tributaries sampled averaged 18.6 cm $h^{-1}$ (excluding a few anomalous values).

Measurements of gas fluxes with floating chambers and calculations based on concentration gradients and *k* values each have methodological issues. Several authors have compared such methodologies and discussed differences between them (e.g., Duchemin 1999; Vachon et al. 2010; Schubert et al. 2012). Floating chambers, even when drifting, can alter near-surface turbulence (Lorke et al. 2015), and short deployment times will not represent the full range of environmental conditions. Chambers shelter the surface from rain or wind-induced waves and cannot be deployed under conditions with high winds and waves. While measurements of near-surface gas concentrations are straightforward and can be automated, calculations of *k* values usually depend on empirical relations with wind speed or currents. As noted by Zappa et al. (2007), *k* values based on formulations using measurements or calculations of the rate of turbulent energy dissipation are theoretically sound and promising. Turbulence within near-surface waters, generated by processes such as convective cooling or internal waves, can be important (MacIntyre et al. 2010; Tedford et al. 2014). Further studies of gas exchange in large rivers using innovative methods and hydrodynamic theory are needed.

Ebullition can increase rates of methane evasion and add variance to the rates. Although floating chambers can capture bubbles and abrupt increases in concentration in chambers with continuous records of methane concentration can be attributed to bubbles (Crill et al. 1988; Bartlett et al. 1990), short deployments and small areas of chambers are likely to lead to under-estimation of ebullition. Another approach is to calculate diffusive fluxes based on surficial concentrations and an appropriate *k* value, and to subtract these values from the total flux captured in the floating chambers. If the *k* selected is too low, the apparent ebullition will be too high, and flux estimates from the 1980s and 1990s generally used low *k* values. To increase spatial and temporal coverage of ebullitve fluxes, submerged funnels are often used (e.g., Kemenes et al. 2007); it was not feasible to deploy funnels in the rivers we sampled, and we spent insufficient time in the lakes to obtain results. Recent applications of hydroacoustic measurements have allowed significant improvements in the estimation of ebullition (Del Sontro et al. 2011), although results from this method have yet to be reported for the Amazon basin.

Sawakuchi et al. (2014) attempted to divide methane fluxes between diffusive and ebullition by assuming the minimum fluxes captured in floating chambers represented diffusive fluxes and that larger fluxes were owed to ebullition in the rivers. However, most of the *k* values derivable for their median values for flux and concentration are within the range discussed above without the need for ebullition. Furthermore, conditions in large Amazonian rivers frequently include episodes of wind-driven waves enhanced by many kilometer fetches, numerous eddy structures on spatial scales from meters to ten of meters, frontal features with converging currents and current generated shear: all conducive to elevated *k* values. Spatial heterogeneity in surficial methane concentrations will lead to further variability in fluxes (Hofmann 2013). Hence, while ebullition may occur in rivers, no direct evidence is available and indirect approaches are likely to be compromised by the wide ranges of *k* expected in turbulent rivers.

**Regional extrapolation**

To extrapolate our diffusive emission values for rivers to river channels throughout the lowland Amazon basin we used the classified open water areas derived from SRTM data (Farr et al. 2007). Based on an examination of these data in comparison to river channels delimited by the open water classification of Hess et al. (2003, 2015) using 100 m resolution synthetic radar data and of Hansen et al. (2013) using Landsat data, the SRTM product represents well large river channels with widths greater than 200 m and less well channels with widths of about 100 m. The SRTM data were acquired during rising water in February which approximates average annual channel areas. We used these data to estimate river channel areas for the major rivers sampled and for the whole lowland basin (Table 6). Melack (still in press) provides a summary and evaluation of other estimates of river channel areas for the Amazon basin.

We combined our areal estimates with our new diffusive fluxes and those of others to estimate basin-specific and total lowland methane emission from channels of large Amazonian rivers (Table 6). Although fluxes were calculated for several major rivers, the sampling was done only in the lower reaches of the rivers, except for the Negro and Solimões/Amazonas rivers. The LW flux determined for the Japura R, was much larger than other measurements and was excluded from the calculation to not unduly influence the extrapolation to the whole river. For the Negro basin, the median values of the modelled LW and HW fluxes were used. The total $CH_4$ diffusive emission for the mainstem rivers and tributaries, including the Solimões and the lower Amazon, with a channel area of 40,710 $km^2$, is 0.24 Tg C $yr^{-1}$. Assuming these values are representative of the river channels in the whole lowland basin with a combined channel area of 52,380 $km^2$, total lowland diffusive emission is estimated as 0.31 Tg C $yr^{-1}$. This methane fluxes represent 1.4% of the

lowland basin-wide methane emission from lakes, floodplains, wetlands, and river of 22 Tg C $yr^{-1}$ calculated by Melack et al. (2004). Stanley et al. (2015) estimated an annual global emission of 26.8 Tg $CH_4$ from streams and rivers.

These estimates include uncertainties caused by sampling and analytical variability as well as systematic problems associated with under-sampling the full extent of diel, episodic, seasonal and inter-annual variations, the small area captured by the floating chambers, issues with the calculation of *k* values, and local to regional differences in the hydrological and ecological conditions. We can quantify only a subset of these uncertainties. The coefficient of variation (CV) for paired chambers in the mainstem Solimões R. ranged from 8% to 45%, and in the tributaries ranged from 6% to 84%. The high values were uncommon, and the average CV for all chamber fluxes measured in the Solimões basin was 30%. For the Negro basin, tributary CVs for chamber fluxes ranged between 5% and 63% with an average of 21%. Mainstem LW chamber fluxes had a CV ranging between 3% and 20% (average of 13%). Melack et al. (2004) applied a Monte Carlo propagation of error analysis that combined error estimates of emissions and inundated areas; for the mainstem Solimões and Amazonas they calculated the standard deviation as a percentage of the annual flux as 13%. The combination of the quantified uncertainties lead to an estimated variation of 20–30% for our 0.24 Tg C $yr^{-1}$, although unquantified spatial and temporal variations would increase the uncertainty. Our lowland basin-wide estimate of 0.31 Tg C $yr^{-1}$ would include even greater uncertainty as it extends into unsampled environments.

Further advances in our estimates of methane emission from the Amazon basin and from other tropical floodplain systems and understanding of the processes involved will require several lines of research. High frequency and time series measurements of emission with chambers and in situ concentrations are now possible with instruments such as cavity ringdown spectrometers (Crawford et al. 2015). Such measurements should be done in under-sampled habitats including flooded forests and within herbaceous vegetation and over 24 h periods for all seasons. Hydroacoustic surveys of bubbling will also provide extensive data on this spatially and temporally variable process. Experimental assays of methane oxidation and production using realistic environmental conditions and appropriate substrates will contribute to improved models. Recent developments of surface renewal models of gas exchange will allow incorporation of physical processes critical to calculations of fluxes (e.g., Tedford et al. 2014).

## References


Abril, G., and others. 2005. Carbon dioxide and methane emissions and the carbon budget of a 10-year old tropical reservoir (Petit Saut, French Guiana). Global Biogeochem. Cycles **19**: 1–16. doi:10.1029/2005GB002457

Abril, G., and others. 2014. Amazon River carbon dioxide outgassing fuelled by wetlands. Nature **505**: 395–398. doi:10.1038/nature12797

Alin, S., M. F. F. L. Rasera, C. I. Salimon, J. E. Richey, G. W. Holtgrieve, A. V. Krusche, and A. Snidvongs. 2011. Physical controls on carbon dioxide transfer velocity and flux in low-gradient river systems and implications for regional carbon budgets. J. Geophys. Res. **116**: G01009. doi:10.1029/2010JG001398

Archer, A. W. 2005. Review of Amazonian depositional systems, p. 17–39. In M. Blum, S. Marriott and S. Leclair [eds.], Fluvial sedimentology. Blackwell Publishing Ltd.

Bartlett, K., P. M. Crill, D. I. Sebacher, R. C. Harriss, J. O. Wilson, and J. Melack. 1988. Methane flux from the central Amazonian floodplain. J. Geophys. Res. **93**: 1574–1582.

Bartlett, K., P. M. Crill, J. Bonassi, J. E. Richey, and R. Harriss. 1990. Methane flux from the Amazon River floodplain: Emissions during rising water. J. Geophys. Res. **95**: 16,773–16,788. doi:10.1029/JD095iD10p16773

Bastviken, D., A. L. Santoro, H. Marotta, L. Pinho, D. Calheiros, P. M. Crill, and A. Enrich-Prast. 2010. Methane emissions from Pantanal, South America, during the low water season: Toward more comprehensive sampling. Environ. Sci. Technol. **44**: 5450–5455. doi:10.1021/es1005048

Beaulieu, J. J., W. D. Shuster, and J. A. Rebholz. 2012. Controls on gas transfer velocities in a large river. J. Geophys. Res. **117**: G02007. doi:10.1029/2011JG001794

Belger, L., B. R. Forsberg, and J. Melack. 2011. Carbon dioxide and methane emissions from interfluvial wetlands in the upper Negro River basin, Brazil. Biogeochemistry **105**: 171–183. doi:10.1007/s10533-010-9536-0

Borges, A. V., and others. 2015a. Divergent biophysical controls of aquatic $CO_2$ and $CH_4$ in the world's two largest rivers. Sci. Rep. **5**. doi:10.1038/srep15614

Borges, A. V., and others. 2015b. Globally significant greenhouse-gas emissions from African inland waters. Nat. Geosci. doi:10.1038/NGEO2486

Bridgham, S., H. Cadillo-Quiroz, K. Kazahaya, and Q. Zhuang. 2013. Methane emissions from wetlands: Biogeochemical, microbial, and modeling perspectives from local to global scales. Glob. Chang. Biol. **19**: 1325–1346. doi:10.1111/gcb.12131

Burnham, K. P., and D. R. Anderson. 2004. Multimodel inference—understanding AIC and BIC in model selection. Sociol. Methods Res. **33**: 261–304. doi:10.1177/0049124104268644

Caraballo, P., B. R. Forsberg, F. Almeida, and R. Leite. 2014. Diel patterns of temperature, conductivity and dissolved oxygen in an Amazon floodplain lake: Description of a *friagem* phenomenon. Acta Limnol. Brasiliensia **26**: 318–331. doi:10.1038/ngeo2486

Cole, J., and N. F. Caraco. 1998. Atmospheric exchange of carbon dioxide in a low-wind oligotrophic lake measured by the addition of SF6. Limnol. Oceanogr. **43**: 647–656. doi:10.4319/lo.1998.43.4.0647

Crawford, J. T., L. C. Loken, N. J. Casson, C. Smith, A. G. Stone, and L. A. Winslow. 2015. High-speed limnology: Using advanced sensors to investigate spatial variability in biogeochemistry and hydrology. Environ. Sci. Technol. **42**: 442–450. doi:10.1021/es504773x.

Crill, P. M., and others. 1988. Tropospheric methane from an Amazonian floodplain lake. J. Geophys. Res. **93**: 1564–1570. doi:10.1029/JD093iD02p01564

Crusius, J., and R. Wanninkhof. 2003. Gas transfer velocities measured at low wind speed over a lake. Limnol. Oceanogr. **48**: 1010–1017. doi:10.4319/lo.2003.48.3.1010

Del Sontro, T., M. J. Kunz, T. Kempter, W. A. B. Wehrli, and D. B. Senn. 2011. Spatial heterogeneity of methane ebullition in a large tropical reservoir. Environ. Sci. Technol. **45**: 9866–9873. doi:10.1021/es2005545

Devol, A., P. D. Quay, J. E. Richey, and L. Martinelli. 1987. The role of gas exchange in the inorganic carbon, oxygen, and $^{222}$Rn budgets of the Amazon River. Limnol. Oceanogr. **32**: 235–248. doi:10.4319/lo.1987.32.1.0235

Devol, A., J. Richey, and W. Clark. 1988. Methane emissions to the troposphere from the Amazon floodplain. J. Geophys. Res. **93**: 1583–1592. doi:10.1029/JD093iD02p01583

Devol, A., J. Richey, B. Forsberg, and L. Martinelli. 1990. Seasonal dynamics in methane emissions from the Amazon River floodplain to the troposphere. J. Geophys. Res. **95**: 417–426. doi:10.1029/JD095iD10p16417

Devol, A., J. Richey, B. Forsberg, and L. Martinelli. 1994. Environmental methane in the Amazon river floodplain, p. 151–165. *In* W. J. Mitsch [ed.], Global wetlands: Old world and new. Elsevier Science.

Duchemin, E. 1999. Comparison of static chamber and thin boundary layer equation methods for measuring greenhouse gas emissions from large water bodies. Environ. Sci. Technol. **33**: 350–357. doi:10.1021/es9800840

Engle, D., and J. Melack. 2000. Methane emissions from an Amazon floodplain lake: Enhanced release during episodic mixing and during falling water. Biogeochemistry **51**: 71–90. doi:10.1023/A:1006389124823

Farr, T. G., and others. 2007. The shuttle radar topography mission. Rev. Geophys. **45**: RG2004. doi:10.1029/2005RG000183

Forster, P., and others. 2007. Changes in atmospheric constituents and in radiative forcing, p. 129–234. *In* S. Solomon and others [eds.], Climate Change 2007: The Physical Science Basis. Contribution of Working Group I to the Fourth Assessment Report of the Intergovernmental Panel on Climate Change. Cambridge Univ. Press.

Golterman, H. L., R. S. Clymo, and M. A. M. Ohnstad. 1978. Methods of physical and chemical analysis of freshwaters. Blackwell.

Hamilton, S., S. Sippel, and J. M. Melack. 1995. Oxygen depletion and carbon dioxide and methane production in waters of the Pantanal wetland of Brazil. Biogeochemistry **30**: 115–141.

Hansch, C., and A. J. Leo. 1979. Substitute constants for correlation analysis in chemistry and biology. Wiley.

Hansen, M. C., and others. 2013. High-resolution global maps of 21st-century forest cover change. Science **342**: 850–853. doi:10.1126/science.1244693

Hess, L. L., J. M. Melack, E. M. L. M. Novo, C. C. F. Barbosa, and M. Gastil. 2003. Dual- season mapping of wetland inundation and vegetation for the central Amazon basin. Remote Sens. Environ. **87**: 404–428. doi:10.1016/j.rse.2003.04.001

Hess, L. L., A. G. Affonso, C. Barbosa, M. Gastil, J. M. Melack, and E. M. L. M. Novo. 2015. Amazonian wetlands: Extent, vegetative cover, and dual season inundation area. Wetlands. **35**: 745–756. doi:10.1007/s13157-015-0666-y

Hofmann, H. 2013. Spatiotemporal distribution patterns of dissolved methane in lakes: How accurate are the current estimations of the diffusive flux path? Geophys. Res. Lett. **40**: 2779–2784. doi:10.1002/grl.50453

Jati, S. R. 2013. Emissão de $CO_2$ e $CH_4$ das savanas úmidas de Roraima. M.Sc. thesis. Instituto Nacional de Pesquisas da Amazônia.

Junk, W. J., M. T. Piedade, J. Schöngart, M. Cohn-Haft, J. M. Adeney, and F. Wittmann. 2011. A classification of major naturally-occurring Amazonian lowland wetlands. Wetlands **31**: 623–640. doi:10.1007/s13157-011-0190-7

Kemenes, A., B. Forsberg, and J. Melack. 2007. Methane release below a tropical hydroelectric dam. Geophys. Res. Lett. **34**: L12809. doi:10.1029/2007GL029479

Kemenes, A., B. Forsberg, and J. Melack. 2011. $CO_2$ emissions from a tropical hydroelectric reservoir (Balbina, Brazil). J. Geophys. Res. Biogeosci. **116**: G03004. doi:10.1029/2010JG001465

Kemenes, A., B. R. Forsberg, and J. M. Melack. 2016. Downstream emissions of $CH_4$ and $CO_2$ from Amazon hydroelectric reservoirs (Tucuruí, Samuel and Curuá-Una) Inland Waters. **6**: 295–302. doi:105268/IW-6.3.980.

Kirschke, S., and others. 2013. Three decades of global methane sources and sinks. Nat. Geosci. **28**: 813–822. doi:10.1038/ngeo1955

Lenth, R. V., and M. Herva. 2015. lsmeans: Least-Squares Means. R package version 2.19.

Lorenzen, C. 1967. Determination of chlorophyll and pheopigments: Spectrophotometric equations. Limnol. Oceanogr. **12**: 343–346. doi:10.4319/lo.1967.12.2.0343

Lorke, A., and others. 2015. Technical note: Drifting vs. anchored flux chambers for measuring greenhouse gas emissions from running waters. Biogeosci. Discuss. **12**: 14619–14645. doi:10.5194/bgd-12-14619-2015

MacIntyre, S., R. Wanninkhof, and J. Chanton. 1995. Trace gas exchange across the air-water interface in freshwater and coastal marine environments, p. 52–97. *In* P. Matson and R. Harriss [eds.], Biogenic trace gases: Measuring emissions from soil and water. Blackwell.

MacIntyre, S., A. Jonsson, M. Jansson, J. Aberg, D. E. Turney, and S. D. Miller. 2010. Buoyancy flux, turbulence, and the gas transfer coefficient in a stratified lake. Geophys. Res. Lett. **37**: L24604. doi:10.1029/2010GL044164.

Mayorga, E., and others. 2005. Young organic matter as a source of carbon dioxide outgassing from Amazonian rivers. Nature **436**: 538–541. doi:10.1038/nature03880

Mazerolle, M. J. 2015. AICcmodavg: Model selection and multimodel inference based on (Q)AIC(c).

Melack, J. M. In press. Aquatic ecosystems. *In* L. Nagy, B. Forsberg and P. Artaxo [eds.], The large-scale biosphere atmosphere programme in Amazonia. Ecological Studies. Springer.

Melack, J., and B. Forsberg. 2001. Biogeochemistry of Amazon floodplain lakes and associated wetlands, p. 235–274. *In* M. McClain, R. Victoria and J. Richey [eds.], The biogeochemistry of the Amazon Basin. Oxford Univ. Press.

Melack, J., and others. 2004. Regionalization of methane emissions in the Amazon Basin with microwave remote sensing. Glob. Chang. Biol. **10**: 530–544. doi:10.1111/j.1365-2486.2004.00763.x

Melack, J., and D. Engle. 2009. An organic carbon budget for an Amazon floodplain lake. Verh. Intern. Verein. Limnol **30**: 1179–1182.

Melton, J. R., and others. 2013. Present state of global wetland extent and wetland methane modeling: Conclusions from a model inter- comparison project (WETCHIMP). Biogeosciences **10**: 753–788. doi:10.5194/bg-10-755-2013

Moreira-Turcq, P., and others. 2013. Seasonal variability in concentration, composition, age, and fluxes of particulate organic carbon exchanged between the floodplain and Amazon River. Global Biogeochem. Cycles **27**: 119–130. doi:10.1002/gbc.20022

Oke, T. R. 1988. Boundary layer climates. Routledge, Boca Raton, Fla.

Paiva, R. C. D., D. C. Buarque, W. Collischonn, M.-P. Bonnet, F. Frappart, S. Calmant, and C. A. Bulhões Mendes. 2013. Large-scale hydrologic and hydrodynamic modeling of the Amazon River basin. Water Resour. Res. **49**: 1226–1243.

Pinheiro, J., B. Douglas, S. DebRoy, D. Sarkar, and R. C Team. 2015. _nlme: Linear and Nonlinear Mixed Effects Models_. R package version 3.1–122.

Polsenaere, P., J. Deborde, G. Detandt, L. O. Vidal, M. A. P. Pérez, V. Marieu, and G. Abril. 2013. Thermal enhancement of gas transfer velocity of $CO_2$ in an Amazon floodplain lake revealed by eddy covariance measurements. Geophys. Res. Lett. **40**: 1734–1740. doi:10.1002/grl.50291

Rasera, M. F. F. L., A. V. Krusche, J. E. Richey, M. V. R. Ballester, and R. L. Victória. 2013. Spatial and temporal variability of *p*CO2 and CO2 efflux in seven Amazonian rivers. Biogeochemistry **116**: 241–259. doi:10.1029/2010JG001465

Raymond, P. A., and others. 2012. Scaling the gas transfer velocity and hydraulic geometry in streams and small rivers. Limnol. Oceanogr. Fluids Environ. **2**: 41–53. doi:10.1215/21573689-1597669

Raymond, P. A., and others. 2013. Global carbon dioxide emissions from inland waters. Nature **503**: 355–359. doi:10.1038/nature12760

Richey, J., A. Devol, S. C. Wofsy, R. Victoria, and M. N. G. Ribeiro. 1988. Biogenic gases and the oxidation and reduction of carbon in Amazon River and floodplain waters. Limnol. Oceanogr. **33**: 551–561. doi:10.4319/lo.1988.33.4.0551

Rosenqvist, Å., B. R. Forsberg, T. Pimentel, Y. A. Rauste, and J. Richey. 2002. The use of spaceborne radar data to model inundation patterns and trace gas emissions in the central Amazon floodplain. Int. J. Remote Sens. **23**: 1303–1328. doi:10.1080/01431160110092911

Rudorff, C., J. Melack, S. MacIntyre, C. C. Barbosa, and E. M. L. Novo. 2011. Seasonal and spatial variability of $CO_2$ emission from a large floodplain lake in the lower Amazon. J. Geophys. Res. Biogeosci. **116**: G04007. doi:10.1029/2011JG001699

Rudorff, C. M., J. M. Melack, and P. D. Bates. 2014a. Flooding dynamics on the lower Amazon floodplain: 1. Hydraulic controls on water elevation, inundation extent, and river-floodplain discharge. Water Resour. Res. **50**: 619–634. doi:10.1002/2013WR014091

Rudorff, C. M., J. M. Melack, and P. D. Bates. 2014b. Flooding dynamics on the lower Amazon floodplain: 2. Seasonal and interannual hydrological variability. Water Resour. Res. **50**: 635–649. doi:10.1002/2013WR014714

Sawakuchi, H., D. Bastviken, A. Krusche, M. V. R. Ballester, and J. E. Richey. 2014. Methane emissions from Amazonian rivers and their contribution to the global methane budget. Glob. Chang. Biol. **20**: 2829–2840. doi:10.1111/gcb.12646

Schubert, C. J., R. Diem, and W. Eugster. 2012. Methane emissions from a small wind shielded lake determined by eddy covariance, flux chambers, anchored funnels, and boundary model calculations: A comparison. Environ. Sci. Technol. **46**: 4515–4522. doi:10.1021/es203465x

Smith, L., W. Lewis, and J. Chanton. 2000. Methane emissions from the Orinoco River floodplain, Venezuela. Biogeochemistry **51**: 113–140. doi:10.1023/A:1006443429909

Stanley, E. H., and others. 2015. The ecology of methane in streams and rivers: Patterns, controls, and global significance. Ecol. Monogr. **86**: 146–171. doi:10.1890/15-1027.1

Tedford, E. W., S. MacIntyre, S. D. Miller, and M. J. Czikowsky. 2014. Similarity scaling of turbulence in a temperate lake during fall cooling. J. Geophys. Res. Oceans **119**: 4689–4713. doi:10.1002/2014JC010135

Teodoru, C. R., F. C. Nyoni, A. V. Borges, F. Darchambeau, I. Nyambe, and S. Bouillon. 2015. Dynamics of greenhouse gases ($CO_2$, $CH_4$, $N_2O$) along the Zambezi River and major tributaries, and their importance in the riverine carbon budget. Biogeosciences **12**: 2431–2453. doi:10.5194/bg-12-2431-2015

Vachon, D., Y. T. Prairie, and J. J. Cole. 2010. The relationship between near-surface turbulence and gas transfer velocity in freshwater systems and its implications for floating chamber measurements of gas exchange. Limnol. Oceanogr. **55**: 1723–1732. doi:10.4319/lo.2010.55.4.1723

Wanninkhof, R. 2014. Relationship between wind speed and gas exchange over the ocean revisited. Limnol. Oceanogr.: Methods **12**: 351–362. doi:10.4319/lom.2014.12.351

Zappa, C. J., and others. 2007. Environmental turbulent mixing controls on air-water gas exchange in marine and aquatic systems. Geophys. Res. Lett. **34**: L10601. doi:10.1029/2006GL028790

## Acknowledgments

The authors thank Bruno Lima for the field support and Marcos Paulo Figueiredo-Barros for discussion, together with the Limnology Lab of the Rio de Janeiro Federal University (Rio de Janeiro and Macaé) for some of the laboratory analysis. This work was supported by Ministério da Ciência Técnologia (CNPq and INCT-INPeTAm/CNPq/MCT), FAPEAM, FINEP, and SECTI. Post-graduate scholarships were provided to P.M.B, V.S and J.H.A. by CNPQ and CAPES. V.F.F is partially supported by grants provided by CNPq. J.M.M received support from NASA.

*Submitted 4 September 2015*
*Revised 2 March 2016; 19 May 2016*
*Accepted 23 May 2016*

*Associate editor: Kimberly Wickland*